Research Article

Chemical Review and Letters
journal homepage: www.chemrevlett.com
ISSN (online): 2645-4947 (print) 2676-7279

Computational investigation on interaction between graphene nanostructure BC_3 and anti-parkinson drug amantadine: Possible sensing study of BC_3 and its doped derivatives on amantadine.

Seyed Jalal Hoseyni[1], Ayda karbakhshzadeh[2, *], Adeleh Moshtaghi Zonouz[2], Beneen Husseen[3,4]

[1]*Department of Chemistry, Shams Gonbad higher education institute, Gonbad kavous, Iran*
[2]*Chemistry Department, Faculty of Science, Azarbaijan Shahid Madani University, Tabriz- Iran. P. O.Box: 53751-71379*
[3]*Medical Laboratory technique college, the Islamic University, Najaf, Iraq*
[4]*Medical laboratory technique college, the Islamic University of Al Diwaniyah, Al Diwaniyah, Iraq*

ARTICLE INFO

Article history:
Received 26 April 2024
Received in revised form 25 May 2024
Accepted 26 May 2024
Available online 30 May 2024

Keywords:
Amantadine
Diamondoid
Sensor
Graphene-like BC_3
Density functional theory (DFT)

ABSTRACT

The purpose of this computational study is to measure and evaluate the interaction between the Parkinson's drug amantadine with BC_3 and its doped nanostructures. The interactions between the diamondoid amantadine molecule and nanosheets including graphene, boron-doped graphene (BC_3), and aluminum, silicon, phosphorus and gallium doped BC_3 have been studied using the B3LYP method with a basis set of 6-31G(d) by Gaussian software 09. A weak interaction energy between the amantadine drug and the graphene nanoparticle was observed. The E_{ad} (adsorption energy) and E_g (gap energy) of BC_3 and Al-, Si-, P-, Ga-doped BC_3 nanosheets with amantadine have been calculated. The results show that graphene nanosheets, BC_3 and its types doped with the mentioned elements cannot be considered as a suitable sensor for the drug amantadine. We conclude that BC_3 nanoparticle doped with the silicon atom shows a good result in terms of HOMO-LUMO difference ($\Delta E_g\% = 90.18$)

1. Introduction

Diamondoids (also called nanodiamonds) are cage saturated hydrocarbon molecules that can be superimposed on the diamond lattice [1]. Thus diamondoids which resemble parts of the diamond lattice, are members of the carbon nanostructure family. The simplest of these diamondoids, with the common name “adamantane”, is a tricyclic $C_{10}H_{16}$ isomer. Diamondoids are very attractive nanoscale building blocks (0.5–2 nm) [2]. The most widely known functionalized adamantane is 1-aminoadamantane (also known as amantadine), which is both an antiviral and anti-parkinson drug [3]. The amino drugs is the important class of the drugs, which use extensively by the people in the world [4-11]. Thus, the detection and sensing these drugs are so serious matter because the release of these drugs damaged the environmental.

The nano structures play a main role in the chemistry with their interesting applications [12-29]. Graphene is a term used to describe very thin strips of graphite monolayers. If we consider graphite as a booklet of parallel sheets, each sheet called graphene. Graphene is called the magic of the 21st century [30, 31]. This material, which is the strongest material studied to date, is said to be a good alternative to silicon. The strange and magical properties of graphene, such as: high electrical conductivity, hardness, very high mechanical strength, excellent optical and surface properties, and high and adjustable thermal conductivity, have made the world of science and media think and research about this material. Graphene known as an electrical conductor in the absence of a band gap. In a graphene sheet, each carbon atom has a free bond outside the sheet [32]. This bond is a good site to put some functional groups as well as hydrogen atoms. The bond between the carbon atoms is covalent and very strong [33,

*Corresponding author.; e-mail: ida.karbakhsh@gmail.com
https://doi.org/10.22034/crl.2024.454413.1328

34]. The BC_3 nanoplate has a geometric structure almost identical to that of graphene nanoplates, except that some of the carbon atoms in the graphene nanoplate have been replaced by boron atoms (so that the carbon atoms are surrounded by boron atoms) to form a nanosheet called BC_3 [35]. It should be noted that the BC_3 nanosheet is an indirect semiconductor with a gap, while the graphene nanosheet is a zero semiconductor. Theoretical research has shown that the electronic properties of the BC_3 nanosheet are amazingly adjustable [36]. At 300 to 600 K the BC_3 monolayer nanosheet can maintain its structure well, even at temperatures above 1000 K it can withstand minor deviations that are not sufficient to destroy the C-C and C-B bonds. If one of the carbon atoms in the BC_3 structure replaced by a nitrogen atom, the structure is displayed as BC_2N. By doping an aluminum, silicon, phosphorus, gallium atoms into BC_3 nanostructure, the doped BC_3 nanosheets can be obtained [37, 38].

2. Computational details

Density functional theory (DFT) is used as a useful computational method for calculating electronic correlations and can often produce MP_2 computational quality results almost simultaneously with the time required for computations (HF) [39]. The energy of the n-electron system can be expressed in terms of the electron probability density. In the DFT method, the electronic energy of the system, based on the Cohen-Sham equation, is written as follows [40, 41].

$$\varepsilon = \varepsilon_T + \varepsilon_V + \varepsilon_J + \varepsilon_{XC} \qquad 1$$

Where ε_T is the expression for kinetic energy that increases with the motion of electrons, and ε_V is the term energy and a potential that includes nucleus-electron and nucleus-nucleus interactions. The term energy ε_J is an electron repulsion - electron ε_{XC}. It is related to the correlation energy and the exchange of electrons [42].
Different DFT methods obtained by combining different types of exchange functions with correlation functions. In this research, in order to optimize the desired complexes, Gaussian09 software has been used [43]. Among the DFT methods, the B_3LYP method is widely used in chemical processes and is used for large molecules and complex systems. In the B_3LYP method, the Beck gradient correction exchange function combined with the Li, Yang, and Par gradient correlation function. In general, in the B_3LYP method, the number 3 indicates the application of three experimental parameters in the Beck exchange function [44]. It is important in the ability of the sensor to be the two factors including energy absorption and the LUMO-HOMO difference. The adsorption energy must be within the suitable range indicating physically range. Besides, if the drug adsorbed on nanoparticles, the LUMO-HOMO difference must reduce until to increase the electrical conductivity of graphene nanoparticles due to the adsorption of amantadine on its outer side forms the BC_3 graphene as a sensor. Our main goal is to use the density density theory (DFT) calculations to theoretically investigate the electrical sensitivity of graphene, BC_3 nanostructures and their doped forms, as well as to investigate whether or not the adsorption and desorption of amantadine molecule on graphene and BC_3 nanosheets are favorable. According to the formula of absorption energy:

$$E_{ad} = E_{\text{adsorption}} = E_{Complex} - E_{nano} - E_{drug} + BSSE \qquad 2$$

Where $E_{(nano)}$ the total energy of the nanosheet, $E_{(drug)}$ total energy of the drug amantadine, $E_{(Amantadine/adsorbent),}$ the total energy of the drug amantadine absorbed on the adsorbent surface and $E_{(BSSE)}$. To get % ΔE_g you have to use the following equation:

$$E_{gap} = E_g = E_{LUMO} - E_{HOMO} \qquad 3$$

$$\% \Delta E_g = (E_{g\text{-complex}} - E_{g\text{-nano}}) / E_{g\text{-nano}} \times 100 \qquad 4$$

The larger the % ΔE_g complex, the greater the nanosheet sensitivity to the drug. As a result, the nanosheet is a good sensor for the drug.

3. Results and Discussion

The absorption of amantadine on nanoparticles is very important. The purpose of this research is the ability of graphene nanoparticle to absorb and detect amantadine and its sensing ability.

In this research, the possible complexes between amantadine drug molecule and graphene nanosheets, BC_3 and the doped with Si, Al, P, Ga atoms considered. The difference in energy levels between HOMO and LUMO indicates the electrical conductivity. To improve the sensing ability of graphene or BC_3 nanosheet, one of the boron atoms of nanosheet BC_3 replaced with the silicon, phosphorus, gallium and aluminum atoms and the resulting absolute energy, bond lengths, HOMO and LUMO investigated.

Table 1. Comparison of energy of raw materials, products and enthalpy changes

Nano structure	E_T(au)	ΔE_T (au)	ΔE_T (kcal.mol)
Amantadine-BC_3	-1567.91518753	-0.01864753	-11.7013
Amantadine-BC_3-Al	-1785.45708058	-0.07400058	-46.4353
Amantadine-BC_3-Si	-1832.55701394	-0.06346394	-39.8236
Amantadine-BC_3-Ga	-3465.96634351	-0.06351351	-39.8547
Amantadine-BC_3-P	-1884.35748725	-0.01535275	-9.6338
Amantadine	-1674.08206918	-0.00042918	-0.2693

Table 2. Comparison of HOMO, LUMO and Hardness Energy for Thirteen Possibilities of Amantadine Approaching Graphene, BC_3 Nanosheets and Doped Derivatives

Nano structure	E_{HOMO}(H)	E_{HOMO}(eV)	E_{LUMO}(H)	E_{LUMO}(eV)	η(H) =εL-εH	η(eV) =εL-εH	%ΔE_g
BC_3	-0.195	-5.30	-0.172	-4.68	0.023	0.62	-
BC_3-Al	-0.195	-5.30	-0.172	-4.68	0.023	0.62	-
BC_3-Si	-0.209	-5.68	-0.149	-4.05	0.06	1.63	-
BC_3-Ga	-0.193	-5.25	-0.170	-4.62	0.023	0.63	-
BC_3-P	-0.197	-5.36	-0.173	-4.70	0.024	0.66	-
Graphene	-0.181	-4.92	-0.073	-1.98	0.108	2.94	-
Amantadine	-0.225	-6.12	-0.068	-1.85	0.157	4.27	-
Amantadine-BC_3	-0.186	-5.06	-0.161	-4.38	0.025	0.68	9.67
Amantadine-BC_3-Al	-0.180	-4.89	-0.155	-4.21	0.025	0.68	9.67
Amantadine-BC_3-Si	-0.194	-5.27	-0.188	-5.11	0.006	0.16	-90.18
Amantadine-BC_3-Ga	-0.181	-4.92	-0.156	-4.24	0.025	0.68	7.93
Amantadine-BC_3-P	-0.167	-4.54	-0.138	-3.75	0.029	0.79	19.69
Amantadine-Graphene	-0.181	-4.94	-0.074	-2.01	0.107	2.93	-0.34

4. Experimental

4.1. Amantadine drug complexes and BC_3 and graphene nanosheets

Complexes which formed by interaction between the drug molecule amantadine and nanosheet are investigated here.

4.1.1. Amantadine complex and graphene nanosheet

The amantadine molecule made the complexes through its amino moiety with the carbon atom of the graphene nanoseet *via* the nitrogen atom (Fig 1). The absorption energy of E_{ad} amantadine and graphene nanosheet is -0.2693 kcal/mol (Table 1). The highest occupied molecular orbital (HOMO) is located at -4.94 eV and the lowest unoccupied molecular orbital (LUMO) is located at -2.01 eV. Thus, E_g is obtained at about 2.93 eV (Table 2). There is a very small difference between the E_g of graphene nanosheets and the E_g of the complex between amantadine and graphene.

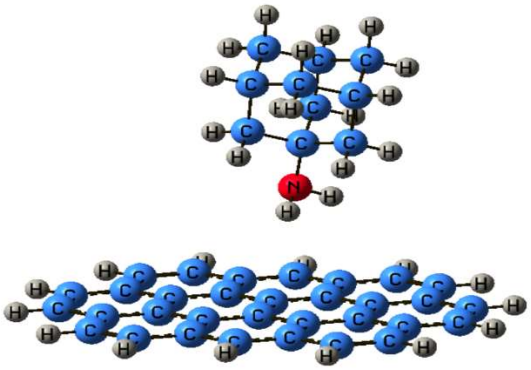

Fig. 1. Optimized structure of amantadine molecule complex with graphene nanosheet.

4.1.2. Amantadine complex and nanosheet BC_3

The nitrogen atom of the amantadine molecule can approach to the boron atom the BC_3 nanoparticle. A complex between the unpaired electron of N atom in amantadine and an empty orbital of the B atom can be formed (Fig 2). The adsorption energy (E_{ad}) in the amantadine-BC_3 complex is -11.70 kcal / mol (Table 1), which is higher than the E_{ad} of the amantadine-graphene complex. The highest occupied molecular orbital (HOMO) is -5.06 and the lowest unoccupied molecular orbital (LUMO) is -4.38 eV. Thus, E_g is obtained 0.68 eV (Table 2). The E_g of the amantadine-BC_3 complex increased from 0.68 to 0.62 eV compared to the BC_3 nanosheet, which is much lower than that of the graphene-amantadine nanosheet.

4.1.3. Amantadine and Al doped-BC_3 nanosheet

The amino group of the amantadine molecule interacts with the aluminum atom of the Al doped-BC_3 nanosheet through the nitrogen atom (Fig 3).

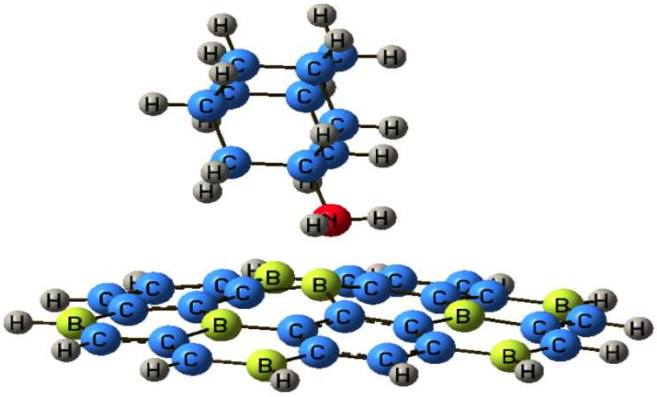

Fig 2. Optimized structure of amantadine molecule complex with BC_3 nanosheet.

The adsorption energy (E_{ad}) in the amantadine-Al doped-BC_3 complex is about -46.43 kcal / mol, which is higher than the E_{ad} of the amantadine-BC_3 complex. Table 1 presents the characteristics of the optimized structure of the amantadine molecule with Al-BC_3 nanosheet. The highest occupied molecular orbital (HOMO) is at -4.89 eV and the lowest unoccupied molecular orbital (LUMO) is at -4.21 eV. Thus, E_g is obtained around eV 0.68 (Table 2). E_g of the amantadine-Al-BC_3 nanosheet complex increased from 0.68 to 0.62 eV compared to the Al doped-BC_3 nanosheet, which is similar to BC_3 nanosheet amantadine complex in terms of $\%\Delta E_g$ difference.

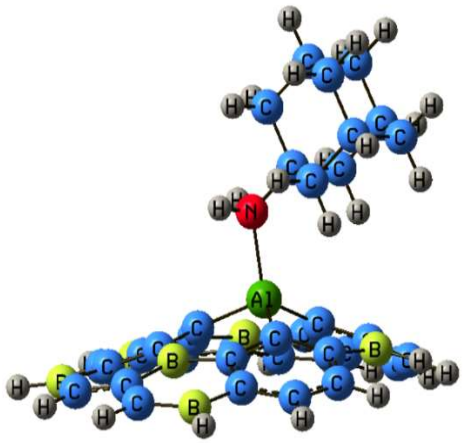

Fig. 3. Optimized structure of amantadine molecule complex with BC_3-Al nanosheet.

4.1.4. Amantadine complex and BC_3-Si nanosheet

The amantadine molecule forms a complex with its BC_3-Si nanosheet silicon atom through its nitrogen atom (Fig 4). The adsorption energy (E_{ad}) in the amantadine-nanosheet complex BC_3-Si is -39.82 kcal / mol, which is less than the E_{ad} of the amantadine-nanosheet BC_3-Al complex. Table 1 presents the specifications of the optimized structure of the amantadine molecule complex with BC_3-Si nanosheet. The highest occupied molecular orbital (HOMO) is at -5.27 eV and the lowest unoccupied molecular orbital (LUMO) is at -5.11 eV. Thus, E_g is obtained at about 0.16 eV (Table2). Amantadine-nanoscript BC_3-Si complex decreased from 0.16 to 1.63 eV compared to BC_3-Si nanosheet, which is much more and more suitable than other complexes. From % ΔE_g point of view, the BC_3-Si nanoplate can be considered suitable as a sensor for the amantadine drug, but this alone is not enough, and for this choice, the absorption energy must also be checked and analyzed.

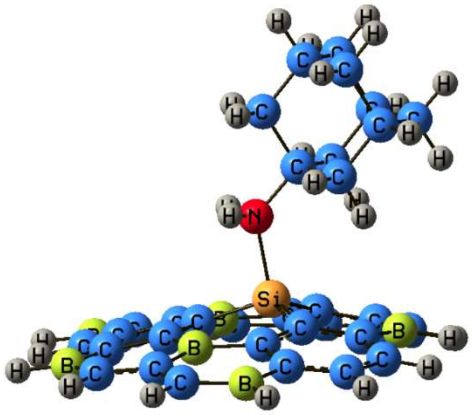

Fig 4. Optimized structure of amantadine molecule complex with BC3-Si nanosheet.

4.1.5. Amantadine complex and BC_3-Ga nanosheet

The amino moiety in amantadine molecule interacts with the gallium atom of the BC_3-Ga nanosheet through its nitrogen atom (Fig 5). The adsorption energy (E_{ad}) in the amantadine-nanosheet complex BC_3-Ga is approximately -39.85 kcal / mol, which is higher than the E_{ad} of the amantadine-nanosheet complex BC_3-Si. Table 1 presents the characteristics of the optimized structure of the amantadine molecule with BC_3-Ga nanosheet. The highest occupied molecular orbital (HOMO) is -4.92 at eV and the lowest unoccupied molecular orbital (LUMO) is -4.24 at eV. Thus, E_g is obtained at about 0.68 eV (Table 2). Thus, E_g is obtained at about 0.68 eV (Table 2). Amantadine-BC_3-Ga nanosheet complex increased from 0.68 to 0.63 eV compared to BC_3-Ga nanosheet, which is very insignificant.

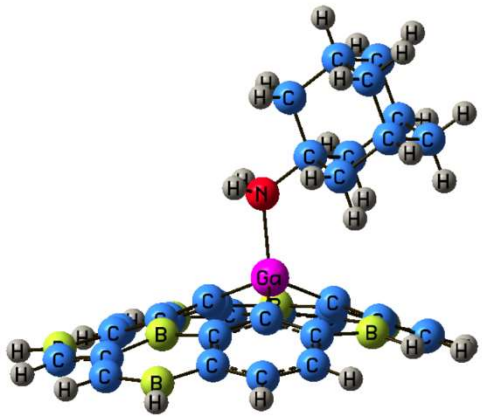

Fig 5. Optimized structure of amantadine molecule complex with BC_3-Ga nanosheet.

4.1.7. Amantadine complex and BC_3-P nanosheet

The amantadine molecule forms a complex with the phosphorus doped-BC_3-P nanosheet through its nitrogen atom (Fig 6). The adsorption energy of E_{ad} in the amantadine-nanosheet complex BC_3-P is -9.363 kcal / mol, which is less than the E_{ad} of the amantadine-nanosheet BC_3-Ga complex. Table 1 presents the characteristics of the optimized structure of the amantadine molecule complex with BC_3-P nanosheet. The highest occupied molecular orbital (HOMO) is at -4.54 eV and the lowest unoccupied molecular orbital (LUMO) is at -3.75 eV. Thus, E_g is obtained at about 0.79 eV (Table2). Amantadine complex of BC_3-P nanosheets increased from 0.79 to 0.66 eV compared to amantadine nanosheet BC_3-P complex, which is not suitable at all.

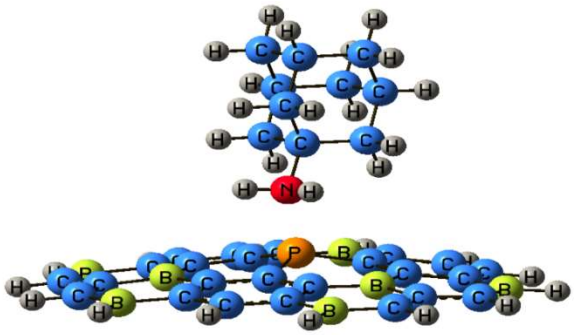

Fig 6. Optimized structure of amantadine molecule complex with BC_3-P nanosheet.

5. conclusion

The interactions between the amantadine molecule and nanoparticles including graphene, BC_3, and doped BC_3 with aluminum, silicon, phosphorus and gallium atoms

Table 3. Amantadine drug molecule and complexes with BC_3 nanoplate and BC_3 doped in terms of HOMO-LUMO energy

name	structure
Amantadine-Graphene	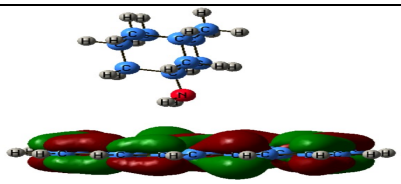 HOMO 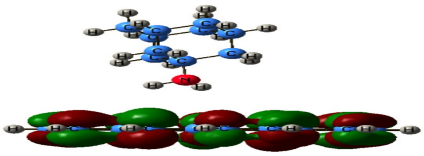 LUMO
Amantadine-BC_3	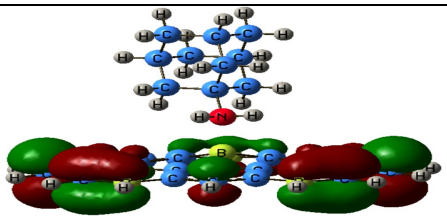 HOMO 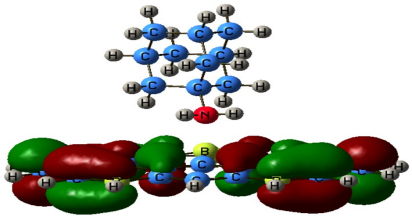 LUMO
Amantadine-BC_3-Al	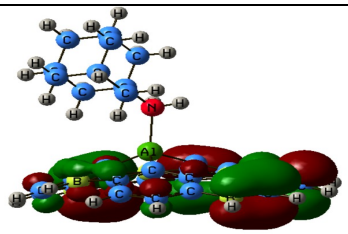 HOMO 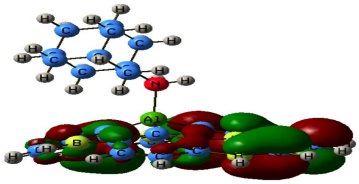 LUMO
Amantadine-BC_3-Si	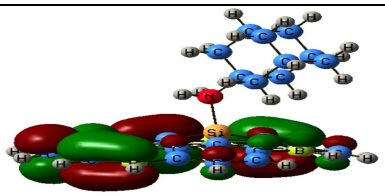 HOMO 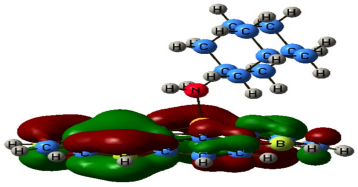 LUMO
Amantadine-BC_3-Ga	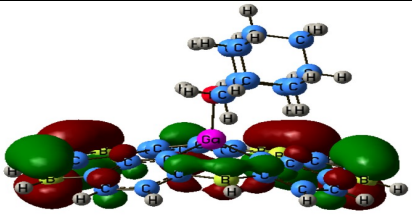 HOMO 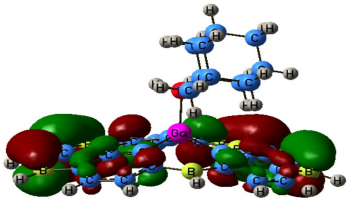 LUMO
Amantadine-BC_3-P	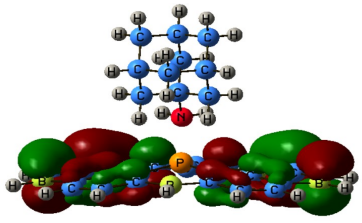 HOMO 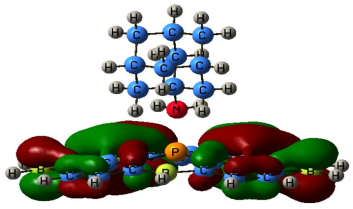 LUMO

have been studied using the B_3LYP method with a basis set of 6-31G(d) by Gaussian software 09. The interaction between the amantadine drug and the graphene nanoparticle show poor energy interactions to amantadine. The interaction between the BC_3 nanosheet and the amantadine drug was also studied. The E_{ad} (adsorption energy) and E_g (gap energy) of BC_3 and doped nanosheet to amantadine were studied.

We conclude that BC_3 nanoparticle doped with the silicon atom shows a good result in terms of HOMO-LUMO difference ($\Delta E_g\% = 90.18$), while in terms of absorption energy, it can be a suitable sensing ability for detecting the amantadine drug only at high temperature.

Acknowledgements

We are grateful for the support of Shahid Madani University of Tabriz, Tabriz University and also Payame Noor University, Tabriz Branch.

References

[1] A. P. Marchand, Diamondoid Hydrocarbons--Delving into Nature's Bounty. *Science*; *299*(5603) (2003) 52-53.

[2] H. Schwertfeger, A. A. Fokin, & P. R. Schreiner, Diamonds are a chemist's best friend: diamondoid chemistry beyond adamantane. *Angewandte Chemie International Edition*, *47*(6) (2008)1022-1036.

[3] D. B. Vu, T. V. Nguyen, S. T. Le, & C. D. Phan, An improved synthesis of amantadine hydrochloride. *Organic Process Research & Development*, *21*(11) (2017) 1758-1760.

[4] R. J. Mohamed, A. K. O. Aldulaimi, S. A. Aowda, Synthesized of new alkaloid compounds and study their anticancer activity. Paper presented at the *AIP Conference Proceedings,* 2660 (2022) 020082. doi:10.1063/5.0108821.

[5] A. K. O. Aldulaimi, A. H. Idan, A. A. Majhool, M. J. Jawad, Z. H. Khudhair, S. M. Hassan, S. S. S. A. Azziz, Synthesis of new antibiotic agent based on mannich reaction. *Int. J. Drug Deliv. Tec., 12*(3) (2022) 1428-1432. doi:10.25258/ijddt.12.3.83.

[6] M. Mosavi, Theoretical study of interaction between Mexiletine drug and pristine, Si-, Ga- and Al-doped boron nitride nano sheet, *J. Chem. Lett.* 3 (2022) 150-158. 10.22034/jchemlett.2023.384082.1103

[7] A. K. Obaid Aldulaimi; E. A. Mahmood; E. Vessally, Sulfaguanidines: A new class of carbonic anhydrase inhibitors, *Med Med Chem,* 1 (2024) 2-9. 10.22034/medmedchem.2024.198914.

[8] A. Karbakhshzadeh, S. Majedi, V. Abbasi, Computational investigation on interaction between graphene nanostructure BC3 and Rimantadine drug: Possible sensing study of BC3 and its doped derivatives on Rimantadine, *J. Chem. Lett.* 3 (2022) 108-113. 10.22034/jchemlett.2022.352857.1079

[9] A. K. O. Aldulaimi, M. J. Jawad, S. M. Hassan, T. S. Alwan, S. S. S. A. Azziz, Y. M. Bakri, The potential antibacterial activity of a novel amide derivative against gram-positive and gram-negative bacteria. *Int. J. Drug Deliv. Tec., 12*(2) (2022) 510-515. doi:10.25258/ijddt.12.2.8.

[10] A. Ajala, A. Uzairu, G. A. Shallangwa, S. E. Abechi, In-silico screening, molecular docking, pharmacokinetics studies and design of histone deacetylase inhibitors as anti-Alzheimer agents, *J. Chem. Lett.* 3 (2022) 38-45.10.22034/jchemlett.2022.335742.1063

[11] A. K. O. Aldulaimi, A. A. Majhool, I. S. Hasan, M. Adil, S. M. Saeed, A. H. Adhab, New MCRs: Preparation of Novel Derivatives of Pyrazoloazepines in Ionic Liquid and Study of Biological Activity, *Polycycl. Aromat. Comp.,* (2023). DOI: 10.1080/10406638.2023.2254903.

[12] A. K. O. Aldulaim, N. M. Hameed, T. A. Hamza, A. S. Abed, The antibacterial characteristics of fluorescent carbon nanoparticles modified silicone denture soft liner. *J. Nanostruct.,* 12 (2022) 774-781. doi:10.22052/JNS.2022.04.001.

[13] M. Y. Saleh, A.K.O. Aldulaimi, S.M. Saeed, A.H. Adhab, TiFe2O4@SiO2–SO3H: A novel and effective catalyst for esterification reaction, *Heliyon*, 4 (2024) https://doi.org/10.1016/j.heliyon.2024.e26286

[14] F. Arjomandi Rad, J. Talat Mehrabad, E. Dargahi Maleki, Synthesis and characterization of Gabapentin-Zn2 Al-LDH nanohybrid and investigation of its drug release and biocompatibility properties on a laboratory scale, J. Chem. Lett. 5 (2024). 10.22034/jchemlett.2024.442139.1157

[15] P. O. Ameh, Removal of Methylene Blue from Aqueous Solution using Nano Metal Oxide Prepared from Local Nigerian Hen Egg Shell: DFT And Experimental Study, *Chem. Rev. Lett.* 6 (2023) 29-43. 10.22034/crl.2023.328721.1155

[16] E. Vessally, M.R. Ilghami, M. Abbasian, Investigation the Capability of Doped Graphene Nanostructure in Magnesium and Barium Batteries with Quantum Calculations, *Chem. Res. Technol.* 1 (2024). 10.2234/chemrestec.2024.436837.1007.

[17] B. Baghernejad, F. Nuhi, A new approach to the facile synthesis of 1,8-dioxooctahydroxanthene using nano-TiO2/ CNT as an efficient catalyst, *Chem. Rev. Lett.* 6 (2022) 268-277. 10.22034/crl.2022.340828.1166

[18] P. O. Ameh, Synthesized iron oxide nanoparticles from Acacia nilotica leaves for the sequestration of some heavy metal ions in aqueous solutions, *J. Chem. Lett.* 4 (2023) 38-51. 10.22034/jchemlett.2023.360137.1083.

[19] H. Ashassi-Sorkhabi, A. Kazempour, J. Mostafaei, E. Asghari, Impact of ultrasound frequency on the corrosion resistance of electroless nickel-phosphorus-nanodiamond

plating, *Chem. Rev. Lett.* 6 (2022) 187-192. 10.22034/crl.2022.345098.1169

[20] Milad. Sheydaei, M. Edraki, Poly(butylene trisulfide)/CNT nanocomposites: synthesis and effect of CNT content on thermal properties, *J. Chem. Lett.* 3 (2022) 159-163. 10.22034/jchemlett.2023.380990.1101.

[21] B. Ghanavati, A. Bozorgian, J. Ghanavati, Removal of Copper (II) Ions from the Effluent by Carbon Nanotubes Modified with Tetrahydrofuran, *Chem. Rev. Lett.* 6 (2022) 68-75. 10.22034/crl.2022.326950.1152

[22] M. Sheydaei, M. Edraki, Vinyl ester/C-MMT nanocomposites: investigation of mechanical and antimicrobial properties, *J. Chem. Lett.* 3 (2022) 95-98. 10.22034/jchemlett.2022.350678.1074.

[23] M. Sheydaei, S. Shahbazi-Ganjgah, E. Alinia-Ahandani, M. Sheidaie, M. Edraki, An overview of the use of plants, polymers and nanoparticles as antibacterial materials, *Chem. Rev. Lett.* 6 (2022) 207-216. 10.22034/crl.2022.343015.1168

[24] P. R. A. Selvan, M. Praveendaniel, Synthesis and Application of TiO2-Phosphomolybdic acid nanocomposite, *J. Chem. Lett.* 4 (2023) 10.22034/jchemlett.2023.395693.1114**.**

[25] S. Arabi, Adsorption of Orange 3R by chitosan modified montmorillonite nanocomposite, *Chem. Rev. Lett.* 6 (2023) 55-65. 10.22034/crl.2023.387842.1208.

[26] B. Mohammadi, M. R. Jalali Sarvestani, A Comparative Computational Investigation on Amantadine Adsorption on the Surfaces of Pristine, C-, Si-, and Ga-doped Aluminum Nitride Nanosheets, *J. Chem. Lett.* 4 (2023) 66-70. 10.22034/jchemlett.2023.388369.1107

[27] G. Lavanya, T. Suvarna, C.P. Vardhani, Structural and Optical Properties of (MgZnO/rGO) , J. Chem. Lett. 4 (2023) 136-147. 10.22034/jchemlett.2023.396420.1116.

[28] C.-Y. Hsu, A. Yadav, S. M. Mohealdeen, Y. A. Abdulsayed, A. H. Adhab, S. Sharma, et al. Computational quantum mechanical investigation of the functionalized AlN nanotube as the smart carriers for levodopa drug delivery, Bulletin of Materials Science, 47 (2024) 1-8.

[29] B. Ajdari, S. A. Vahed, Fullerene (C20) as a sensing material for electrochemical detection of Nortriptyline: A theoretical study, *J. Chem. Lett.* 3 (2022) 164-168.10.22034/jchemlett.2023.385007.1104

[30] M. J. Allen, V. C. Tung, & R. B. Kaner, Honeycomb carbon: a review of graphene. *Chem. Rev. 110* (2010) 132-145.

[31] D. R. Dreyer, R. S. Ruoff, & C. W. Bielawski, From conception to realization: an historial account of graphene and some perspectives for its future. *Angewandte Chemie International Edition*, *49*(49) (2010) 9336-9344.

[32] S. Park, & R. S. Ruoff, Chemical methods for the production of graphenes. *Nature nanotechnology*, *4*(4) (2009) 217-224.

[33] S. Y. Zhou, G. H. Gweon, A. V. Fedorov, P. D. First, W. A. De Heer, D. H. Lee, ... & A. Lanzara, Substrate-induced bandgap opening in epitaxial graphene. *Nature materials*, *6*(10) (2007) 770-775.

[34] I. A. Popov, & A. I. Boldyrev, Deciphering chemical bonding in a BC_3 honeycomb epitaxial sheet. *The Journal of Physical Chemistry C*, *116*(4) (2012) 3147-3152.

[35] F. C. Chuang, Z. Q. Huang, W. H. Lin, M. A. Albao, & W. S. Su, Structural and electronic properties of hydrogen adsorptions on BC_3 sheet and graphene: a comparative study. *Nanotechnology*, *22*(13) (2011) 135703.Jensen, F., *Introduction to computational chemistry*. John wiley & sons: 2017.

[36] D. C. Young, A practical guide for applying techniques to real-world problems. *Computational Chemistry, New York*, *9* (2001) 390.

[37] E. G. Lewars, & E. G. Lewars, Semiempirical calculations. *Computational Chemistry: Introduction to the Theory and Applications of Molecular and Quantum Mechanics*, (2011) 391-444.

[38] T. Van Mourik, M. Bühl, & M. P. Gaigeot, (2014). Density functional theory across chemistry, physics and biology. *Philosophical Transactions of the Royal Society A: Mathematical, Physical and Engineering Sciences*, *372*(2011) (2014) 20120488.

[39] D. R. Salahub, R. Fournier, P. Młynarski, I. Papai, A. St-Amant, & J. Ushio, Gaussian-based density functional methodology, software, and applications. In *Density functional methods in chemistry* New York, NY: Springer New York. (1991) pp. 77-100.

[40] M. Austin-Seymour, I. Kalet, J. McDonald, S. Kromhout-Schiro, J. Jacky, S. Hummel, & J. Unger, Three dimensional planning target volumes: a model and a software tool. *International Journal of Radiation Oncology* Biology* Physics*, *33*(5) (1995) 1073-1080.

[41] S. Landa, & V. Macháček, Sur l'adamantane, nouvel hydrocarbure extrait du naphte. *Collection of Czechoslovak Chemical Communications*, *5* (1933) 1-5.

[42] V. L. Deringer, A. P. Bartók, N. Bernstein, D. M. Wilkins, M. Ceriotti, & G. Csányi, Gaussian process regression for materials and molecules. *Chemical Reviews*, *121*(16) (2021) 10073-10141.

[43] Y. Qiu, & S. R. White, Hybrid gausslet/Gaussian basis sets. *The Journal of Chemical Physics*, (2021) *155*(18).

[44] R. Lindh, & I. F. Galván, Molecular structure optimizations with Gaussian process regression. In *Quantum Chemistry in the Age of Machine Learning* (pp. 391-428). Elsevier.